

Chemistry of a Ni(II) Acetohydroxamic Acid Complex: Formation, Reactivity with Water, and Attempted Preparation of Zinc and Cobalt Analogues

Katarzyna Rudzka,[†] Atta M. Arif,[‡] and Lisa M. Berreau^{*†}

Department of Chemistry and Biochemistry, Utah State University, Logan, Utah 84322-0300, and Department of Chemistry, University of Utah, Salt Lake City, Utah 84112

Received May 19, 2005

Mononuclear Ni(II), Co(II), and Zn(II) complexes of the bppppa (*N,N*-bis[(6-phenyl-2-pyridyl)methyl]-*N*-[(6-pivaloylamido-2-pyridyl)methyl]amine) ligand have been synthesized and characterized by X-ray crystallography, ¹H NMR, UV–vis (Ni(II) and Co(II)) and infrared spectroscopy, and elemental analysis. Each complex has the empirical formula [(bppppa)M](ClO₄)₂ (M = Ni(II), **2**; Zn(II), **3**; Co(II), **4**) and in the solid state exhibits a metal center having a coordination number of five; albeit, the cation of **2** also has a sixth weak interaction involving a perchlorate anion. Treatment of [(bppppa)Ni](ClO₄)₂ (**2**) with 1 equiv of acetohydroxamic acid results in the formation of [(bppppa)-Ni(HONHC(O)CH₃)](ClO₄)₂ (**1**), a novel Ni(II) complex having a coordinated neutral acetohydroxamic acid ligand. In **1**, one phenyl-appended pyridyl donor of the bppppa chelate ligand is dissociated from the metal center and acts as a hydrogen bond acceptor for the hydroxyl group of the bound acetohydroxamic acid ligand. Treatment of **1** with excess water results in the formation of **2** and free acetohydroxamic acid. We hypothesize that this reaction occurs due to disruption of the intramolecular hydrogen bonding interaction involving the bound acid. In this series of reactions, the bppppa ligand exhibits behavior reminiscent of a type III hemilabile ligand in terms of one phenylpyridyl donor. Treatment of **3** or **4** with acetohydroxamic acid results in no reaction, indicating that the bppppa-ligated Ni(II) derivative **2** exhibits unique coordination chemistry with respect to reaction with acetohydroxamic acid within this series of complexes. We attribute this reactivity to the ability of the bppppa-ligated Ni(II) center to adopt a pseudo-octahedral geometry, whereas the Zn(II) and Co(II) complexes retain five coordinate metal centers.

Introduction

Recently we reported the synthesis and characterization of a novel mononuclear Ni(II) complex containing a neutral bidentate acetohydroxamic acid ligand, [(bppppa)Ni(HONHC(O)CH₃)](ClO₄)₂ (**1**, Figure 1).¹ A phenyl-appended pyridyl moiety of the supporting chelate ligand (bppppa, *N,N*-bis-[(6-phenyl-2-pyridyl)methyl]-*N*-[(6-pivaloylamido-2-pyridyl)methyl]amine) in **1** accepts a hydrogen bond from the hydroxyl group of the Ni(II)-coordinated acid. Complex **1** is interesting in that while structurally characterized examples of d-block metal complexes of the acetohydroxamate anion

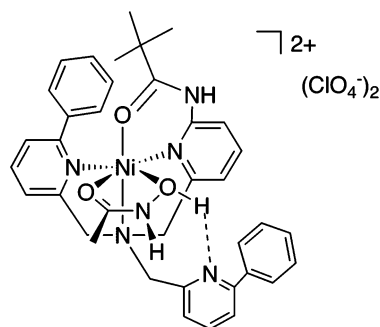


Figure 1. Drawing of [(bppppa)Ni(HONHC(O)CH₃)](ClO₄)₂ (**1**).

(AHA[−]) are common, particularly for Ni(II),^{2–5} Zn(II),^{5–7} and Co(II),^{5,8} complex **1** represents the first example of a synthetic complex wherein neutral acetohydroxamic acid (AHA) ligation has been identified. Notably, neutral acetohydroxamic acid coordination at a single Ni(II) center has

* To whom correspondence should be addressed. E-mail: berreau@cc.usu.edu. Phone: (435) 797-1625. Fax: (435) 797-3390.

[†] Utah State University.

[‡] University of Utah.

(1) Rudzka, K.; Makowska-Grzyska, M. M.; Szajna, E.; Arif, A. M.; Berreau, L. M. *Chem. Commun.* **2005**, 489–491.

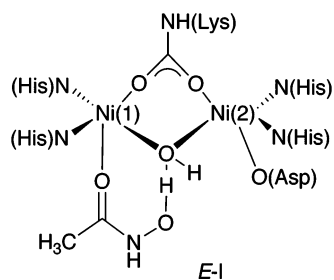


Figure 2. E-I species proposed to form in urease enzymes from *Klebsiella aerogenes* and *Bacillus pasteurii*.

been suggested for a weak enzyme/inhibitor complex (E-I) formed within the active site of urease enzymes obtained from *Klebsiella aerogenes* and *Bacillus pasteurii* (Figure 2).^{9–11} Stabilization of this E-I species may involve a hydrogen bonding interaction with the bridging hydroxyl group.¹¹

In the experiments reported herein, we have examined the formation of **1** from a Ni(II) precursor complex, [(bppppa)-Ni](ClO₄)₂ (**2**). Paramagnetic ¹H NMR and UV–vis measurements indicate that quantitative formation of **1** from **2** occurs in the presence of only a single equivalent of acetohydroxamic acid. However, the acid ligand of **1** can be displaced in the presence of water to regenerate **2** and free acetohydroxamic acid. Spectroscopic investigation of the reactivity of Zn(II) and Co(II) analogues of **2** with acetohydroxamic acid revealed no evidence for formation of neutral acid-bound complexes of these metals.

Experimental Section

General Methods. All reagents and solvents were obtained from commercial sources and used as received without further purification. The bppppa (*N,N*-bis[(6-phenyl-2-pyridyl)methyl]-(6-pivaloylamido-2-pyridyl)methyl)amine ligand was prepared according to the literature procedure.¹

Physical Methods. Diamagnetic ¹H and ¹³C NMR spectra were collected using a Bruker ARX-400 spectrometer. Paramagnetic ¹H NMR spectra were recorded as previously described.¹² UV–vis spectra of **1**, **2**, and **4** were recorded at ambient temperature using a Hewlett-Packard 8453 diode array spectrophotometer. Solid-state

infrared spectra were recorded on a Shimadzu FTIR-8400 spectrometer as KBr pellets. Elemental analyses were performed by Atlantic Microlabs of Norcross, GA.

Caution: Perchlorate salts of metal complexes with organic ligands are potentially explosive. Only small amounts of material should be prepared, and these should be handled with great care.¹³

General Method for Preparation of 2–4. Stirring of a methanol solution of the bppppa ligand (~0.06 mmol in ~4 mL of methanol) with a molar equivalent amount of the appropriate metal perchlorate salt (M(ClO₄)₂·6H₂O, M = Ni, Zn, and Co), followed by removal of the solvent under reduced pressure and recrystallization via Et₂O diffusion into a CH₃CN/CH₃OH solution of the residue yielded the perchlorate complexes in >70% yield as single crystals suitable for X-ray crystallographic analysis.

[(bppppa)Ni](ClO₄)₂ (2**).** Yield: 72%. UV–vis, nm (ε, M⁻¹ cm⁻¹): 572 (20), 890 (26). FTIR (KBr, cm⁻¹): 3354 (ν_{N–H}), 1620, 1099 (ν_{ClO₄}), 621 (ν_{ClO₄}). Anal. Calcd for C₃₅H₃₅N₅O₉Cl₂Ni: C, 52.69; H, 4.43; N, 8.78. Found: C, 52.62; H, 4.22; N, 8.74.

[(bppppa)Zn](ClO₄)₂ (3**).** Yield: 82%. ¹H NMR (CD₃CN, 400 MHz): δ 8.82 (br s, 1H), 8.22–8.13 (m, 3H), 7.80 (d, *J* = 7.2 Hz, 2H), 7.61 (d, *J* = 7.6 Hz, 2H), 7.47–7.42 (m, 4H), 7.38–7.34 (m, 4H), 7.27–7.25 (m, 4H), 4.58–4.43 (m, 6H), 0.54 (s, 9H). ¹³C-¹H NMR (CD₃CN, 100 MHz): δ 185.4, 160.5, 157.6, 153.5, 152.7, 144.8, 143.3, 139.2, 131.5, 130.6, 129.0, 127.2, 124.6, 122.7, 117.7, 57.1, 56.7, 42.1, 26.7 (19 signals expected and observed). FTIR (KBr, cm⁻¹): 3352 (ν_{N–H}), 1622, 1105 (ν_{ClO₄}), 621 (ν_{ClO₄}). Anal. Calcd for C₃₅H₃₅N₅O₉Cl₂Zn: C, 52.16; H, 4.38; N, 8.69. Found: C, 52.29; H, 4.32; N, 8.68.

[(bppppa)Co](ClO₄)₂ (4**).** Yield: 76%. UV–vis, nm (ε, M⁻¹ cm⁻¹): 470 (110), 590 (50), 725 (30). FTIR (KBr, cm⁻¹): 3433 (ν_{N–H}), 1618, 1105 (ν_{ClO₄}), 623 (ν_{ClO₄}). Anal. Calcd for C₃₅H₃₅N₅O₉Cl₂Co: C, 52.62; H, 4.42; N, 8.77. Found: C, 52.63; H, 4.38; N, 8.67.

X-ray Crystallography. Crystals of **2–4** were each mounted on a glass fiber with viscous oil and then transferred to a Nonius KappaCCD diffractometer with Mo Kα radiation (λ = 0.71073 Å) for data collection at 150(1) K. The methodology used for determination of final unit cell constants has been previously reported.¹² For the data collected for **2–4**, each reflection was indexed, integrated, and corrected for Lorentz, polarization, and absorption effects using DENZO-SMN and SCALEPAC.¹⁴ All of the non-hydrogen atoms of **2–4** were refined with anisotropic displacement coefficients.

Structure Solution and Refinement. Complexes **2–4** all crystallize in the space group *P* $\bar{1}$. For **2** and **4**, all hydrogen atoms were located and refined independently using SHELXL97.¹⁵ For **3**, all hydrogens except the amide proton were assigned isotropic displacement coefficients (*U*(H) = 1.2*U*(C) or 1.5*U*(C_{methyl})), and their coordinates were allowed to ride on their attached carbons using SHELXL97. The amide proton of **3** was located and refined independently.

Results

Synthesis. To more fully investigate the coordination chemistry related to the formation and reactivity of the novel acetohydroxamic acid complex [(bppppa)Ni(HONHC(O)-CH₃)](ClO₄)₂ (**1**), a Ni(II) complex of the bppppa chelate ligand, [(bppppa)Ni](ClO₄)₂ (**2**), was prepared as shown in

- (2) Stemmler, A. J.; Kampf, J. W.; Kirk, M. L.; Pecoraro, V. L. *J. Am. Chem. Soc.* **1995**, *117*, 6368–6369.
- (3) Arnold, M.; Brown, D. A.; Deeg, O.; Errington, W.; Haase, W.; Herlihy, K.; Kemp, T. J.; Nimir, H.; Werner, R. *Inorg. Chem.* **1998**, *37*, 2920–2925.
- (4) Jedner, S. B.; Schwöppe, H.; Nimir, H.; Rempel, A.; Brown, D. A.; Krebs, B. *Inorg. Chim. Acta* **2002**, *340*, 181–186.
- (5) Makowska-Grzyska, M. M.; Szajna, E.; Shipley, C.; Arif, A. M.; Mitchell, M. H.; Halfen, J. A.; Berreau, L. M. *Inorg. Chem.* **2003**, *42*, 7472–7488.
- (6) Hammes, B. S.; Kieber-Emmons, M. T.; Letizia, J. A.; Shirin, Z.; Carrano, C. J.; Zakharov, L. N.; Rheingold, A. L. *Inorg. Chim. Acta* **2003**, *346*, 227–238.
- (7) Puerta, D. T.; Cohen, S. M. *Inorg. Chem.* **2002**, *41*, 5075–5082.
- (8) Brown, D. A.; Errington, W.; Glass, W. K.; Haase, W.; Kemp, T. J.; Nimir, H.; Ostrovsky, S. M.; Werner, R. *Inorg. Chem.* **2001**, *40*, 5962–5971.
- (9) Todd, M. J.; Hausinger, R. P. *Microbiol. Rev.* **1989**, *53*, 85–108.
- (10) Pearson, M. A.; Michel, L. O.; Hausinger, R. P.; Karplus, P. A. *Biochemistry* **1997**, *36*, 8164–8172.
- (11) Benini, S.; Rypniewski, W. R.; Wilson, K. S.; Miletto, S.; Ciurli, S.; Mangani, S. *J. Biol. Inorg. Chem.* **2000**, *5*, 110–118.
- (12) Szajna, E.; Dobrowolski, P.; Fuller, A. L.; Arif, A. M.; Berreau, L. M. *Inorg. Chem.* **2004**, *43*, 3988–3997.

(13) Wolsey, W. C. *J. Chem. Educ.* **1973**, *50*, A335–A337.

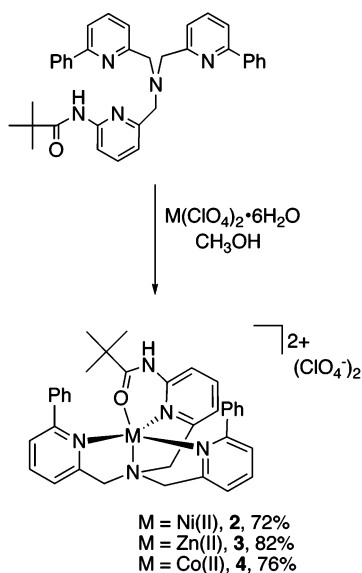
(14) Otwinowski, Z.; Minor, W. *Methods Enzymol.* **1997**, *276*, 307–326.

(15) Sheldrick, G. M. *SHELXL-97, Program for the Refinement of Crystal Structures*; University of Göttingen: Germany, 1997.

Table 1. Summary of X-ray Data Collection and Refinement^a

	2	3	4
empirical formula	C ₃₅ H ₃₅ Cl ₂ N ₅ O ₉ Ni	C ₃₅ H ₃₅ Cl ₂ N ₅ O ₉ Zn	C ₃₅ H ₃₅ Cl ₂ N ₅ O ₉ Co
formula weight	799.29	805.95	799.51
crystal system	triclinic	triclinic	triclinic
space group	<i>P</i> $\bar{1}$	<i>P</i> $\bar{1}$	<i>P</i> $\bar{1}$
<i>a</i> (Å)	11.1285(3)	11.1799(3)	11.1919(2)
<i>b</i> (Å)	11.7383(4)	11.8178(2)	11.7809(2)
<i>c</i> (Å)	14.7611(2)	14.6539(4)	14.6419(3)
α (deg)	87.7231(16)	86.8463(15)	86.6445(13)
β (deg)	70.8954(14)	70.8582(12)	70.8059(11)
γ (deg)	67.5294(12)	67.8369(13)	67.9376(11)
<i>V</i> (Å ³)	1675.63(8)	1688.68(7)	1685.06(5)
<i>Z</i>	2	2	2
density, calcd (Mg m ⁻³)	1.584	1.585	1.576
temp (K)	150(1)	150(1)	150(1)
color	purple	colorless	green
crystal habit	plate	plate	plate
crystal size (mm ³)	0.40 × 0.38 × 0.15	0.30 × 0.20 × 0.05	0.35 × 0.28 × 0.08
diffractometer	Nonius KappaCCD	Nonius KappaCCD	Nonius KappaCCD
abs coeff (mm ⁻¹)	0.805	0.951	0.734
2 θ max (deg)	54.92	54.96	54.96
completeness to 2 θ (%)	99.2	98.5	99.3
reflections collected	11376	11176	12467
indep reflections	7601 [R(int) = 0.0179]	7627 [R(int) = 0.0264]	7677 [R(int) = 0.0254]
variable parameters	610	476	610
R1/wR2 ^b	0.0332/0.0740	0.0417/0.0852	0.0384/0.0786
goodness-of-fit (<i>F</i> ²)	1.043	1.071	1.070
largest diff (e Å ⁻³)	0.340/−0.473	0.379/−0.530	0.478/−0.382

^a Radiation used: Mo K α (λ = 0.71073 Å). ^b R1 = $\sum||F_o| - |F_c||/\sum|F_o|$; wR2 = $[\sum[w(F_o^2 - F_c^2)^2]/\sum(F_o^2)]^{1/2}$ where $w = 1/[\sigma^2(F_o^2) + (aP)^2 + bP]$.

Scheme 1

Scheme 1. For complementary reactivity studies, Zn(II) ([*(bppppa)*Zn](ClO₄)₂, **3**) and Co(II) ([*(bppppa)*Co](ClO₄)₂, **4**) analogues were generated in a similar fashion. Complexes **2–4** were isolated as crystalline solids via recrystallization from CH₃CN/CH₃OH/Et₂O solutions in yields that consistently exceeded 70%.

X-ray Crystallography. Part I. Parameters associated with the data collection and refinement of the X-ray structures of **2–4** are given in Table 1. Selected bond distances and angles are given in Table 2.

[*(bppppa)*Ni](ClO₄)₂ (**2**). An ORTEP representation of the cationic portion of **2**, along with one ClO₄[−] anion, is shown in Figure 3a. The Ni(II) ion has a coordination

Table 2. Selected Bond Distances (Å) and Angles (deg)

	2	3	4
M–N(2)	1.9945(15)	2.0667(19)	2.0441(17)
M–N(3)	2.0427(14)	2.1500(2)	2.1431(17)
M–N(4)	2.0676(15)	2.0758(19)	2.0819(16)
M–N(5)	2.1051(15)	2.1030(2)	2.0971(16)
M–O(1)	1.9563(12)	1.9696(16)	1.9640(14)
N(2)–M–N(4)	106.93(6)	110.69(8)	110.14(6)
N(4)–M–N(5)	108.51(6)	112.89(8)	112.49(7)
N(2)–M–N(5)	137.77(6)	126.03(7)	125.12(7)
O(1)–M–N(2)	90.41(5)	88.64(7)	89.54(6)
O(1)–M–N(4)	107.91(5)	114.86(7)	115.30(6)
O(1)–M–N(5)	99.78(5)	100.31(7)	101.68(6)
O(1)–M–N(3)	170.39(6)	164.04(7)	165.22(6)
N(2)–M–N(3)	84.03(6)	80.03(8)	79.66(7)
N(4)–M–N(3)	81.28(6)	79.93(8)	78.21(6)
N(5)–M–N(3)	79.41(6)	77.86(8)	76.94(6)

geometry that may be described as intermediate between square pyramidal and trigonal bipyramidal (τ = 0.54).¹⁶ Notably, the largest angular distortion from 120° within the pseudoequatorial plane is found in the N(2)–Ni(1)–N(5) bond angle (137.77(6)°). This expanded angle is bisected by a weak interaction involving a perchlorate oxygen atom (Ni(1)···O(7) 2.975 Å). The Ni–O(amide) bond is ~0.08 Å shorter than the corresponding bond in **1**.¹ In addition, the average Ni–N_{PhPy} distance in **2** (2.086 Å) is shorter than the Ni–N_{PhPy} interaction in **1** (Ni(1)–N(4) 2.128(3) Å)¹ and notably shorter than the Ni–N_{PhPy} distances in [(6-Ph₂TPA)Ni(O₂NHC(O)CH₃)]ClO₄ (2.2630(17) and 2.2292(17) Å, Figure 4a) and [(6-Ph₂TPA)Ni(CH₃CN)(CH₃OH)](ClO₄)₂·CH₃OH (2.200(5) and 2.218(5) Å, Figure 4b).⁵ Following a similar trend, the bonding interactions involving the Ni(II) center of **2** and the tertiary amine nitrogen and amide-

(16) Addison, A. W.; Rao, T. N.; Reedijk, J.; van Rijn, J.; Verschoor, G. *C. J. Chem. Soc., Dalton Trans.* **1984**, 1349–1356.

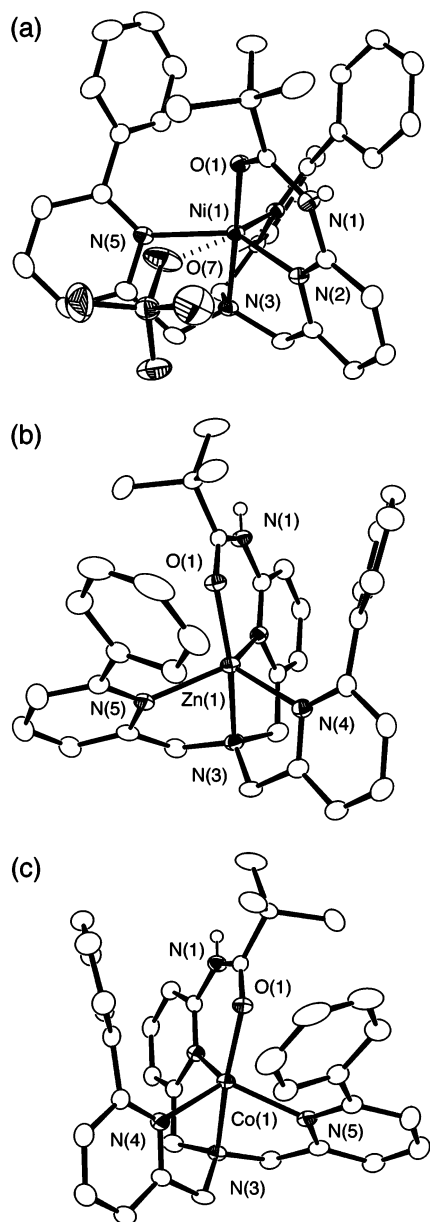


Figure 3. ORTEP representations of the cationic portions of **2–4**. For all, ellipsoids are plotted at the 50% probability level and hydrogen atoms, except the amide N–H proton, have been omitted for clarity.

appended pyridyl donor are both contracted relative to the same interactions in **1**. In sum, these differences indicate an enhanced Lewis acidity for the five-coordinate Ni(II) center of **2** versus the six-coordinate Ni(II) centers found in **1**, [(6-Ph₂TPA)Ni(OHNC(O)CH₃)]ClO₄ (Figure 4a), and [(6-Ph₂TPA)Ni(CH₃CN)(CH₃OH)](ClO₄)₂·CH₃OH (Figure 4b).¹⁵

In the solid-state structure of **2**, a *tert*-butyl methyl group is positioned to form weak CH/π interactions with the phenyl appendages of the bppppa ligand (C(3)⋯arene centroid 3.95 and 3.80 Å).¹⁷ While a similar interaction is not present in **1**, where the shortest C(methyl)⋯arene centroid distance is 4.26 Å, CH/π interactions involving the methyl group of a Ni(II)-bound CH₃CN ligand have been identified in [(6-Ph₂TPA)Ni(CH₃CN)(CH₃OH)](ClO₄)₂·CH₃OH (C(methyl)⋯arene centroid, 3.66 and 3.63 Å, Figure 4b).

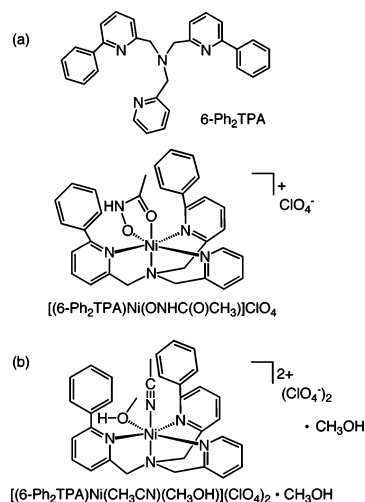


Figure 4. Drawings of 6-Ph₂TPA, (a) [(6-Ph₂TPA)Ni(OHNC(O)CH₃)]ClO₄, and (b) [(6-Ph₂TPA)Ni(CH₃CN)(CH₃OH)](ClO₄)₂·CH₃OH.

Solution Characterization of [(bppppa)Ni(HONHC(O)CH₃)](ClO₄)₂ (1**) and [(bppppa)Ni](ClO₄)₂ (**2**).** (a) **Paramagnetic ¹H NMR.** Recently we reported the solution characterization of a number of pseudo-octahedral 6-Ph₂TPA and TPA-ligated (TPA = tris((2-pyridyl)methyl)amine) Ni(II) complexes using paramagnetic ¹H NMR.¹² In that work, we used a variety of deuterated ligand derivatives, as well as ²H NMR and two-dimensional ¹H–¹H COSY spectra, to assign the ¹H NMR resonances of the supporting chelate ligands. As shown in Figure 5a, we were able to clearly assign the β-H resonances (protons on meta positions) of the pyridyl rings in [(6-Ph₂TPA)Ni(CH₃CN)(CH₃OH)](ClO₄)₂ in the region of ~39–60 ppm. The β and β′ designations differentiate the pyridyl (β) and phenylpyridyl (β′) donors in **1**. Notably, a similar, albeit more complex, set of resonances is observed for **1** under identical conditions (Figure 5b). We assign the resonances at 63.7, 53.9, 38.7, and 34.9 ppm in **2** as β- or β′-H’s on the basis of similarity in chemical shift to the β/β′-H’s of [(6-Ph₂TPA)Ni(CH₃CN)(CH₃OH)](ClO₄)₂·CH₃OH, as well as other Ni(II) derivatives of 6-Ph₂TPA and TPA ligands.¹² However, unlike the β- and β′-H resonances of [(6-Ph₂TPA)Ni(CH₃CN)(CH₃OH)](ClO₄)₂·CH₃OH, which appear in a 1:2:1:2 relative intensity ratio, the four sharpest signals assigned as β/β′-H resonances for **1** appear with a 1:1:1:1 integrated relative intensity. This can be explained by the fact that all three pyridyl rings are inequivalent for **1** and that these four sharp signals represent the β/β′-H protons of only two of the pyridyl rings. The β-H resonances of the third pyridyl ring remain to be identified. However, we hypothesize that this missing set of β-H resonances for **1** is for the noncoordinated phenylpyridyl donor that is involved in the hydrogen bonding interaction with the bound acetohydroxamic acid. Because these protons are positioned further from the nickel center than the other pyridyl β/β′-H’s, their ¹H NMR signals are likely in or near the diamagnetic region, which is obscured by additional ligand and solvent resonances.

(17) Nishio, M.; Hirota, M.; Umezawa, Y. *The CH/π Interaction: Evidence, Nature and Consequences*; Wiley-VCH: New York, 1998.

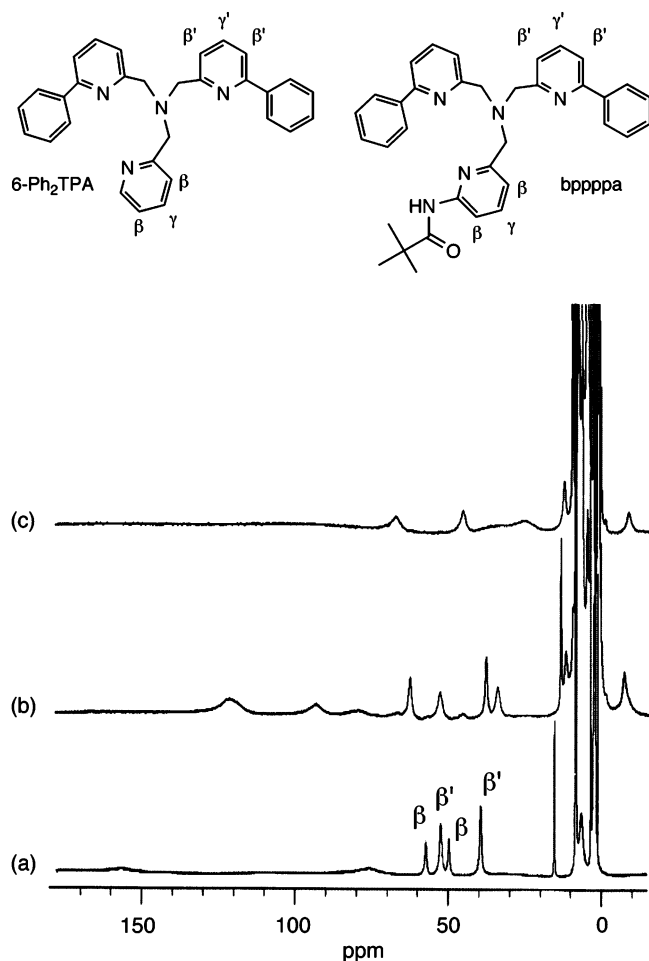


Figure 5. Paramagnetic ^1H NMR spectra of (a) $[(6\text{-Ph}_2\text{TPA})\text{Ni}(\text{CH}_3\text{CN})\text{-(CH}_3\text{OH)}](\text{ClO}_4)_2$,¹² (b) **1**, and (c) **2**. All spectra were collected in dry $\text{CD}_3\text{-CN}$ solution at 25(1) $^\circ\text{C}$.

For **2**, which has a five-coordinate Ni(II) center in the solid state (with a weak sixth perchlorate oxygen interaction), the paramagnetic ^1H NMR features of the complex in dry $\text{CD}_3\text{-CN}$ are strikingly different from those of **1** and other pseudo-octahedral Ni(II) complexes that we have investigated.¹² First, there are only two cleanly identifiable β -type resonances at 68.0 and 46.3 ppm, respectively. These signals exhibit a 1:1 integrated intensity ratio. Several additional broad features are present in the range of $\sim 0\text{--}40$ ppm, which have not been assigned.

Notably, both **1** and **2** exhibit a resonance upfield of 0 ppm (Figure 5b and c). On the basis of the fact that these signals disappear in the presence of D_2O , they are assigned

Scheme 2

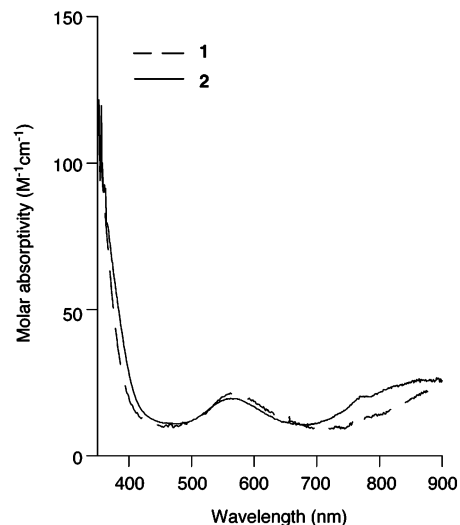
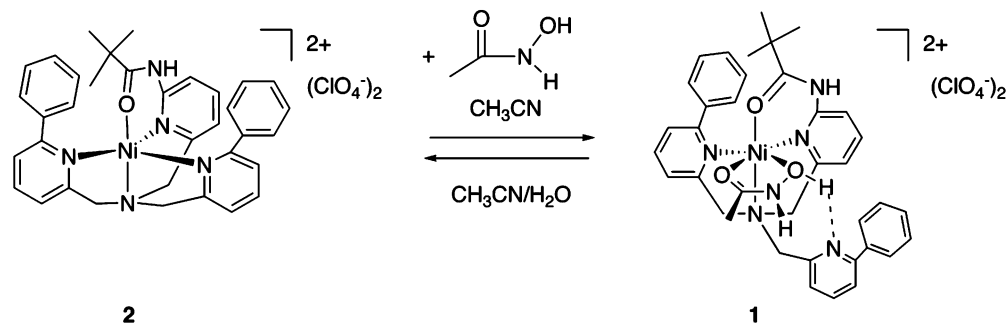


Figure 6. Electronic absorption spectroscopic features of **1** and **2**.

as the amide N–H protons in these complexes. Addition of a large excess of D_2O (~ 600 equiv) to a CD_3CN solution of the acetohydroxamic acid complex **1** also produces additional changes consistent with the release of the acid ligand (vide infra).

Importantly, these preliminary paramagnetic ^1H NMR studies indicate that **1** and **2** exhibit unique paramagnetic ^1H NMR signatures that may be used, in conjunction with complementary electronic absorption spectroscopic experiments (vide infra), to monitor the solution reactivity of **2** with acetohydroxamic acid, a reaction that results in the formation of **1**.

(b) Electronic Absorption Spectroscopy. The electronic absorption spectroscopic properties of **2** are subtly different from those of **1**, as shown in Figure 6, thus giving a secondary technique with which to monitor reactions involving these complexes. In particular, the $^3\text{A}_{2g} \rightarrow ^3\text{T}_{2g}(\text{F})$ transition at ~ 890 nm in **2** is shifted into the near-IR region in **1**.¹⁸

Reactivity of 2 with Acetohydroxamic Acid Resulting in the Formation of 1. Evaluation by Paramagnetic ^1H NMR and Electronic Absorption Spectroscopy. Treatment of $[(\text{bppppa})\text{Ni}](\text{ClO}_4)_2$ (**2**) with 1 equiv of acetohydroxamic acid in CD_3CN solution results in spectral changes in the paramagnetic ^1H NMR consistent with the formation of the acetohydroxamic acid complex, **1** (Scheme 2). As shown in Figure 7, the formation of $[(\text{bppppa})\text{Ni}(\text{HONHC}(\text{O})\text{CH}_3)](\text{ClO}_4)_2$ (**1**, Figure 7b) is indicated by the appearance of four

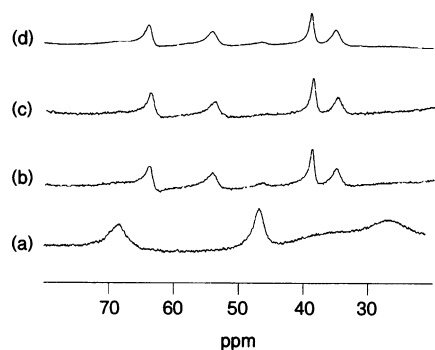


Figure 7. β -H region of the paramagnetic ^1H NMR spectra of (a) **2**, (b) **2** in the presence of 1 equiv of acetohydroxamic acid, (c) **2** in the presence of 2 equiv of acetohydroxamic acid, and (d) analytically pure **1**. All spectra were recorded at 25(1) $^\circ\text{C}$ in CD_3CN .

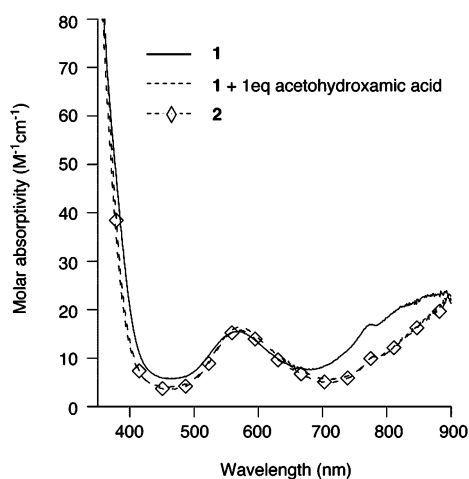


Figure 8. Electronic absorption spectroscopic changes produced upon treatment of **2** with 1 equiv of acetohydroxamic acid. These changes produce an absorption spectrum (dashed line) that is indistinguishable from that observed for analytically pure **1** in CH_3CN solution (dashed line with diamond-shaped markers).

β -H resonances of equal intensity in the region of 30–70 ppm. The chemical shifts of these resonances exactly match those observed for analytically pure **1** under identical conditions (Figure 7d). Formation of **1** appears to be complete upon the addition of 1 equiv of acetohydroxamic acid to **2** (Scheme 2), as the addition of a second equivalent of acetohydroxamic acid results in no additional changes in the observed ^1H NMR features (Figure 7c). As shown in Figure 8, electronic absorption spectroscopic changes produced upon treatment of **2** with 1 equiv of acetohydroxamic acid also indicate the clean formation of **1**.

Displacement of Acetohydroxamic Acid from 1 Occurring in the Presence of Water to Yield 2. Treatment of **1** with excess equivalents of water results in ^1H NMR spectroscopic changes (Figure 9a–d) that indicate the displacement of the acetohydroxamic acid ligand from **1** and the formation of **2**. As shown in Figure 9b, addition of 100 equiv of D_2O to a CD_3CN solution of **1** yields subtle spectral changes in the β -H region as compared to those observed for analytically pure $[(\text{bppppa})\text{Ni}(\text{HONHC}(\text{O})\text{CH}_3)](\text{ClO}_4)_2$ (**1**) under identical conditions (Figure 9a). Addition of

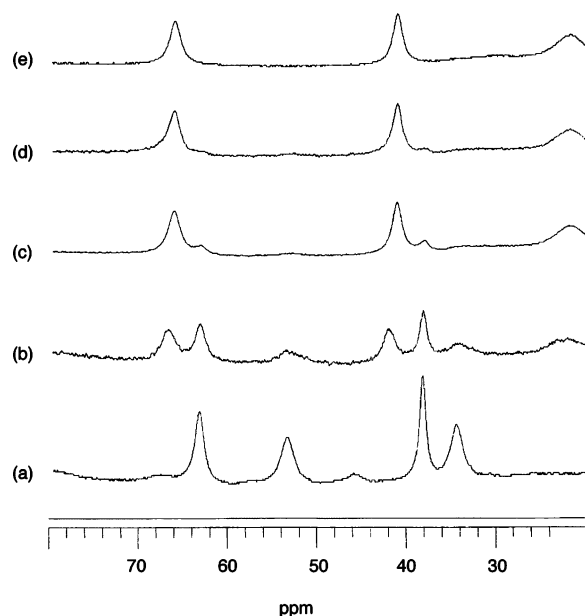


Figure 9. (a) Spectrum of the β -H region of the paramagnetic ^1H NMR spectrum of **1** in CD_3CN at 25(1) $^\circ\text{C}$. (b–d) Spectra of this solution plus (b) 100 equiv, (c) 350 equiv, and (d) 600 equiv of D_2O . (e) Spectrum for analytically pure **2** in CD_3CN containing 600 equiv of D_2O .

increasing equivalents of water, up to 600 equiv total (Figures 9c and d), results in the generation of a paramagnetic ^1H NMR spectrum identical to that exhibited by analytically pure **2** under identical conditions (Figure 9e). Examination of the diamagnetic region of these same spectra (Figure 10) supports a similar interpretation. This conclusion is further supported by the fact that precipitation of analytically pure **1** from a $\text{CH}_3\text{CN}/\text{acetone}/\text{water}$ ($\sim 20\%/ \sim 10\%/ 70\%$) solution, followed by recrystallization of the precipitated solid from $\text{CH}_3\text{CN}/\text{Et}_2\text{O}$, yields crystalline **2**. The identification of this crystalline solid as **2** was confirmed by X-ray crystallographic determination of the unit cell parameters, which matched those previously determined for **2**.

As shown in Scheme 2, these results indicate hemilabile behavior for the supporting bppppa ligand when coordinated to Ni(II).^{19,20} In the presence of acetohydroxamic acid, the five-coordinate Ni(II) complex **2** undergoes dissociation of one of the phenyl-appended pyridyl donors, resulting in stabilization of the acetohydroxamic acid complex **1** via an intramolecular hydrogen bonding interaction. However, in the presence of excess water, the acetohydroxamic acid ligand is displaced and complex **2** is regenerated.

Will Acetohydroxamic Acid Complexes Form with Other d-Block Metals? Evaluation of the Reactivity of Zn(II) and Co(II) Analogues of 2 with Acetohydroxamic Acid. To our knowledge, **2** is the first d-block metal complex to be reported that reacts with acetohydroxamic acid to produce an isolable metal complex having a neutral, coordinated acetohydroxamic acid ligand.¹ To test whether this reactivity will be common in other d-block metal complexes of the bppppa chelate ligand, we have generated Zn(II)

(18) Lever, A. B. P. *Inorganic Electronic Spectroscopy*, 2nd ed.; Elsevier: Amsterdam, 1984.

(19) Slone, C. S.; Weinberger, D. A.; Mirkin, C. A. *Prog. Inorg. Chem.* **1999**, *48*, 233–350.

(20) Braunstein, P.; Naud, F. *Angew. Chem., Int. Ed.* **2001**, *40*, 680–699.

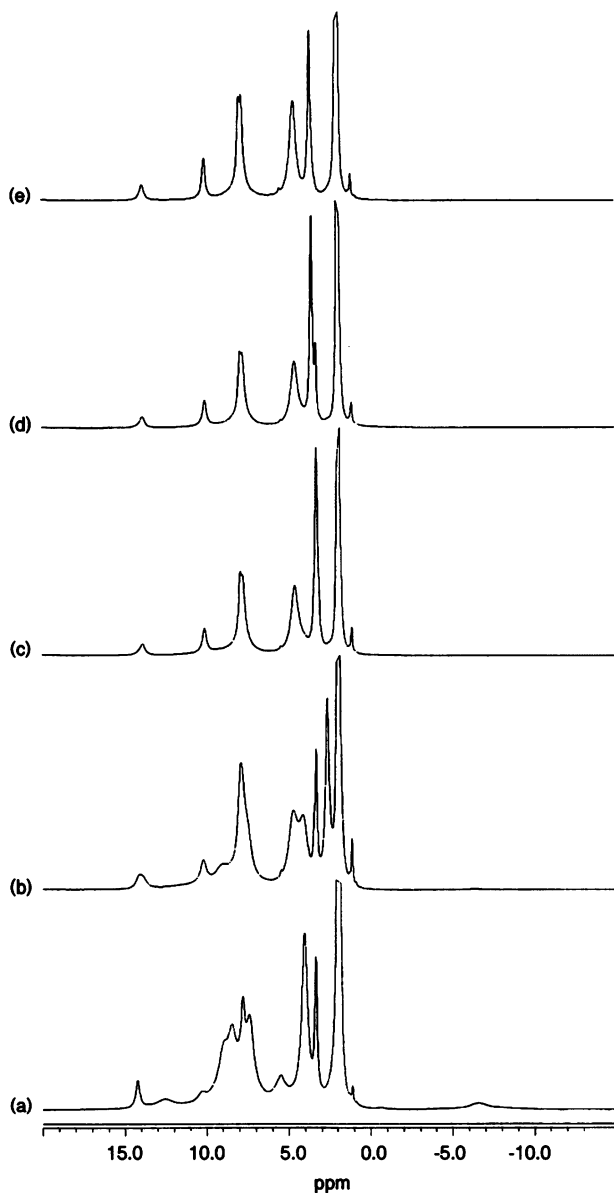


Figure 10. (a) Spectrum of a selected region of the paramagnetic ^1H NMR spectrum of **1** in CD_3CN at $25(1)^\circ\text{C}$. (b–d) Spectra of this solution plus (b) 100 equiv, (c) 350 equiv, and (d) 600 equiv of D_2O . (e) Spectrum for analytically pure **2** in CD_3CN containing 600 equiv of D_2O .

([(bppppa)Zn](ClO_4) $_2$, **3**) and Co(II) [(bppppa)Co](ClO_4) $_2$, **4**) analogues of **2**. These two d-block metals were chosen because of their propensity to form acetohydroxamate complexes.^{5–8}

X-ray Crystallography. Part II. The cationic portions of **3** and **4** are shown in Figure 3b and c. As with the Ni(II) derivative (**2**), the metal centers of **3** and **4** both exhibit an overall coordination number of five. Within each cation, there are weak CH/π interactions akin to those found for **2**.¹⁷ The geometry of the cations of **3** and **4** is best described as distorted trigonal bipyramidal (**3**: $\tau = 0.63$; **4**: $\tau = 0.67$).¹⁶ As previously noted, the Ni(II) center of **2** is of an intermediate geometry between square pyramidal and trigonal bipyramidal ($\tau = 0.54$). Key structural differences for the zinc and cobalt cations versus the nickel analogue (**2**) are the following: (a) a subtle decrease in the linearity of the

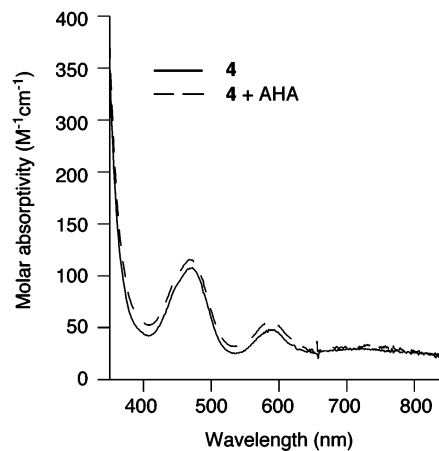


Figure 11. Electronic absorption spectra of **4**. The solid line is the electronic absorption spectrum of **4** in CH_3CN at $25(1)^\circ\text{C}$. The dashed line is the absorption spectrum of **4** in the presence of 10 equiv of acetohydroxamic acid.

$\text{O}(1)\text{--M--N}(3)$ interaction, (b) a more acute equatorial $\text{N}_{\text{AmPy}}\text{--M--N}_{\text{PhPy}}$ angle (e.g., **2**: $\text{N}(2)\text{--Ni--N}(5)$ 137.77° . **3**: $\text{N}(2)\text{--Zn--N}(5)$ 126.03°), and (c) more open $\text{N}(2)\text{--M--N}(4)$ ($\sim 110^\circ$) and $\text{N}(4)\text{--M--N}(5)$ ($\sim 112^\circ$) bond angles in the equatorial plane for the cations of **3** and **4**. In addition, for the Zn(II) and Co(II) complexes, no interaction is found between the cation and either of the perchlorate anions. Thus, the nickel derivative (**2**) is unique within this subset of complexes in that it has a weak sixth interaction involving a perchlorate anion. This interaction, which bisects the $\text{N}(2)\text{--Ni--N}(5)$ angle, provides a rationale for the differences in the equatorial bond angles of **3** and **4** versus those of **2**, as described above.

Solution Characterization of [(bppppa)Zn](ClO_4) $_2$ (3**) and [(bppppa)Co](ClO_4) $_2$ (**4**) in the Absence and Presence of Acetohydroxamic Acid.** The ^1H NMR features of **3** in CD_3CN solution at $25(1)^\circ\text{C}$ are given in the Experimental Section. The most notable ^1H NMR feature of this complex is an upfield shift of the *tert*-butyl methyl protons of the supporting bppppa chelate ligand (**3**: 0.56 ppm) relative to the chemical shift position of this signal for the free ligand (1.24 ppm). This shielding effect may be attributed to the weak CH/π interaction between the *tert*-butyl methyl protons and the phenyl appendages of the bppppa ligand, as noted in the solid-state structure of **3**.¹⁷

Addition of excess acetohydroxamic acid (10 equiv) to a CD_3CN solution of **3** results in the appearance of new signals at ~ 9.1 , 7.6, and 1.8 ppm. These resonances are at chemical shifts consistent with the presence of free acetohydroxamic acid in CD_3CN solution. No changes were found in terms of the multiplicity or chemical shifts of the resonances of **3** in the presence of the acid. This indicates that no reaction takes place between the zinc complex and acetohydroxamic acid.

The Co(II) complex **4** exhibits three electronic transitions (470 (110), ~ 590 (50), and 725 (30) nm; Figure 11) with extinction coefficients consistent with a five-coordinate Co(II) center for **4** in CH_3CN solution.¹⁸ Measurement of the absorption spectrum of **4** in the presence of 10 equiv of acetohydroxamic acid in CH_3CN produced no change in the

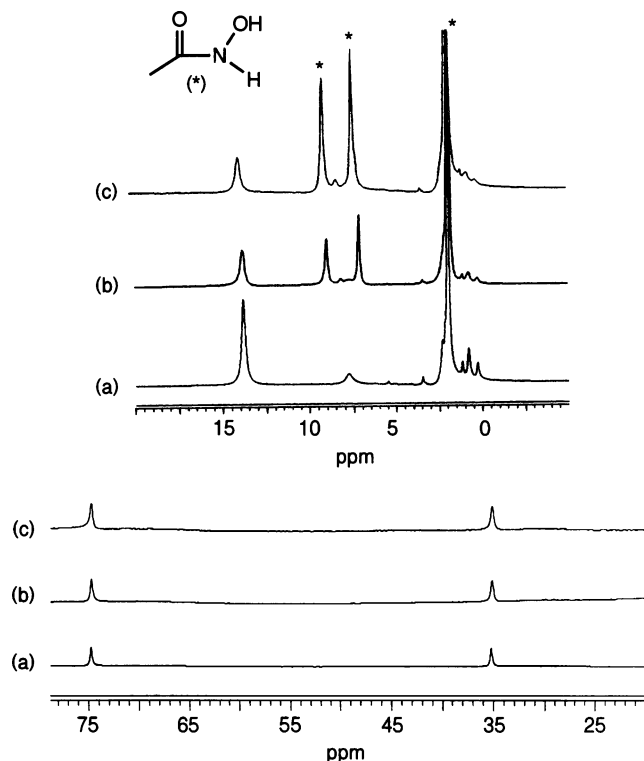


Figure 12. (a) Spectra showing features of the paramagnetic ^1H NMR spectrum of **4** in CD_3CN at $25(1)^\circ\text{C}$. (b and c) Spectra showing (a) with 10 and 20 equiv of acetohydroxamic acid added, respectively. The resonances labeled with * indicate the presence of free acetohydroxamic acid. The solvent residual proton resonance is found at 1.94 ppm.

intensity or wavelength of the electronic transitions, suggesting that no reaction occurs.

Paramagnetic ^1H NMR can also be used to probe the solution reactivity of $\text{Co}(\text{II})$ compounds.²¹ Shown in Figure 12a are the features found in two different regions of the paramagnetic ^1H NMR spectrum of **4**. Assignment of selected resonances has been performed on the basis of the integrated intensity and comparison of spectral features to assigned resonances of structurally related mononuclear $\text{Co}(\text{II})$ complexes.²¹ Two sharp signals at 74.9 and 35.2 ppm, respectively, are assigned as the β -H's of the phenyl-appended pyridyl rings. A ^1H - ^1H COSY spectrum of **4** (data not shown) indicates that these signals are coupled to a γ -H (para to the pyridyl nitrogen) resonance at 0.26 ppm. The *tert*-butyl methyl resonance is present at 13.8 ppm. A signal at -15.6 ppm disappears in the presence of D_2O and is assigned as the amide N-H resonance for **4**.

In parts b and c of Figure 12 are the NMR spectra produced upon treatment of **4** with 10 and 20 equiv of acetohydroxamic acid, respectively. Similar to the electronic absorption spectroscopic results, the NMR data indicates that no reaction occurs between **4** and the acid.

Discussion

We recently reported the isolation and structural characterization of $[(\text{bppppa})\text{Ni}(\text{HONHC}(\text{O})\text{CH}_3)](\text{ClO}_4)_2$ (**1**).¹ This

complex has biological relevance, as neutral acetohydroxamic acid coordination has been suggested for a weak enzyme/inhibitor (E-I) complex involving the active site nickel cluster of urease.⁹⁻¹¹ From a coordination chemistry perspective, **1** is unique in being the first reported example of a d-block metal complex having a coordinated neutral acetohydroxamic acid ligand.²² In the work described herein, we have performed experiments to probe the formation and reactivity of **1** in acetonitrile solution. Formation of **1** from a five-coordinate $\text{Ni}(\text{II})$ precursor complex, $[(\text{bppppa})\text{Ni}](\text{ClO}_4)_2$ (**2**), and 1 equiv of acetohydroxamic acid occurs readily at ambient temperature. The paramagnetic ^1H NMR and electronic absorption spectroscopic features of **1** and **2** differ sufficiently so that $\text{Ni}(\text{II})$ coordination of the acetohydroxamic ligand is easily identifiable.

Potentially tetradentate tris((pyridyl)methyl)amine-type ligands with an aryl or alkyl appendage in the α position of a pyridyl ring have been previously shown to exhibit tridentate coordination modes in $\text{Fe}(\text{II})$ and $\text{Fe}(\text{III})$ complexes, with an α -functionalized pyridyl donor dissociated from the metal center.²³⁻²⁵ In **1**, a noncoordinated phenyl-appended pyridyl donor acts as a hydrogen bond acceptor for the coordinated acetohydroxamic acid ligand.¹ The structural parameters of this hydrogen bonding interaction indicate that it may be classified as moderate and involves an energy of 4–14 kcal/mol.^{1,26} A similar hydrogen bonding interaction was identified in a $\text{Mn}(\text{II})$ complex of the 6-Ph₂-TPA ligand, wherein a noncoordinated phenyl-appended pyridyl nitrogen atom acts as a hydrogen bond acceptor for a metal-coordinated methanol ligand.⁵

Treatment of **1** with excess water results in the release of acetohydroxamic acid and formation of **2**, a complex that does not have a coordinated water ligand. Our hypothesis is that the presence of water disrupts the intramolecular hydrogen bonding interaction involving the coordinated acetohydroxamic acid ligand. This disruption could produce a structure in which coordination of the hydroxamic acid is thermodynamically disfavored with respect to release of the neutral acid and formation of **2**.

The binding of the acid to **2** to form **1** involves behavior of the *bppppa* ligand that is reminiscent of a type III hemilabile ligand, as defined by Braunstein and Naud.²⁰ Specifically, type III hemilabile behavior (Figure 13a) involves coordination of an external reagent that results in the breaking of a labile metal–ligand bond.²⁰ Typical type III hemilabile systems involve CO or another gaseous reactant (e.g., CO_2 or SO_2) as the external reagent, and the reversibility of the reaction results simply from a change in the partial pressure of the gas. In the reaction to produce **1**

(22) A search of the Cambridge Crystallographic Database (version 5.26, with update February 2005) found no examples of neutral acetohydroxamic acid coordination to a d-block metal center.

(23) Mandon, D.; Nopper, A.; Litrol, T.; Goetz, S. *Inorg. Chem.* **2001**, *40*, 4803–4806.

(24) Mandon, D.; Machkour, A.; Goetz, S.; Welter, R. *Inorg. Chem.* **2002**, *41*, 5364–5372.

(25) Jo, D.-H.; Chiou, Y.-M.; Que, L., Jr. *Inorg. Chem.* **2001**, *40*, 3181–3190.

(26) Jeffrey, G. A. *An Introduction to Hydrogen Bonding*; Oxford University Press: New York, 1997.

(21) Tubbs, K. J.; Szajna, E.; Bennett, B.; Halfen, J. A.; Watkins, R. W.; Arif, A. M.; Berreau, L. M. *J. Chem. Soc., Dalton Trans.* **2004**, 2398–2399.

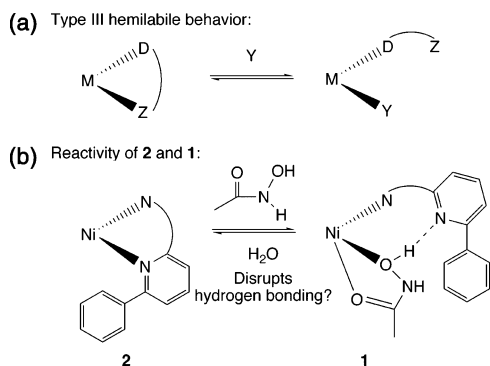


Figure 13. (a) Type III hemilabile ligand behavior as defined by Braunstein and Naud.²⁰ (b) Reactivity properties of **2** and **1**.

from **2**, the dissociated ligand appendage is a phenyl-appended pyridyl moiety that accepts a hydrogen bond from the bound acid (Figure 13 (bottom)). The introduction of water results in release of the acid. As discussed above, we hypothesize that this involves water acting to disrupt the intramolecular hydrogen bonding interaction. These results indicate that coordination of a neutral acetohydroxamic acid ligand to a Ni(II) center, even when stabilized via an intramolecular hydrogen bonding interaction, is susceptible to displacement in the presence of water. Thus, a neutral acetohydroxamic acid adduct in a biological system, such as is proposed to occur in the weak enzyme/inhibitor (E-I) complex of urease, could be disrupted in the presence of water.

As outlined above, Zn(II) and Co(II) analogues of **2** do not form complexes having a neutral acetohydroxamic acid ligand, even in the presence of a large excess of the acid. We rationalize this lack of reactivity in terms of coordination number preferences for the bppppa-ligated metal centers. Specifically, whereas the Ni(II) complex **2** forms a sixth weak interaction with a perchlorate anion in the solid state and exhibits a geometry approximately halfway between square pyramidal and trigonal bipyramidal, the Zn(II) and Co(II) complexes (**3** and **4**) have strictly five-coordinate distorted trigonal bipyramidal metal centers. On the basis of these data, it appears that the key to forming the acetohydroxamic acid complex, **1**, is the ability of the nickel center to form a sixth interaction and adopt a pseudo-octahedral geometry.

Acknowledgment. This work was supported the National Science Foundation (CAREER Award CHE-0094066) and the National Institutes of Health (1R15GM072509). The authors thank Ewa Szajna and Amy Fuller for assistance with selected experiments.

Supporting Information Available: X-ray crystallographic (CIF) files for **2–4**. This material is available free of charge via the Internet at <http://pubs.acs.org>.

IC0508122